Supplementary information: Heat current rectification and mobility edges

Vinitha Balachandran,[1] Stephen R. Clark,[2,3,4] John Goold,[5] and Dario Poletti[1]

[1]*Science and Math Cluster and EPD Pillar, Singapore University of Technology and Design, 8 Somapah Road, 487372 Singapore*
[2]*H.H. Wills Physics Laboratory, University of Bristol, Bristol BS8 1TL, UK.*
[3]*Department of Physics, University of Bath, Claverton Down, Bath BA2 7AY, U.K.*
[4]*Max Planck Institute for the Structure and Dynamics of Matter, University of Hamburg CFEL, Hamburg 22761, Germany.*
[5]*School of Physics, Trinity College Dublin, Dublin 2, Ireland.*

I. STABILITY OF THE RECTIFICATION TO THE PHASE PARAMETER

It is important to show that the effect of the mobility edge on the rectification is robust to changes of the quasi-periodic potential phase parameter ϕ. We thus study the rectification $\mathcal{R}$ versus α for $\phi = \pi$ (red $\diamond$) in Fig. S1, and the average rectification for ϕ chosen from a uniform distribution between $\pi \pm \pi/20$ (blue $\circ$) and $\pi \pm \pi/10$ (green $\square$). The average rectification is computed taking 100 samples of ϕ. We observe that, while noise in the value of the phase ϕ lowers the rectification and makes the jump close to $\alpha = 0$ less steep, the average rectification is robust even to variations of 10% of the mean value.

II. LOCALIZATION PROPERTIES OF THE STEADY STATE

The link between rectification and localization is further unravelled by examining more closely a representative case with $\lambda = 0.9$ and $\alpha = 0.9$. In Fig. S2(a) we report the inverse participation ratio $I(k)$ for the energy eigenmodes, highlighting the mobility edge above which $I(k)$ becomes sizeable indicating localized eigenstates. The NESS eigenmode occupation $\langle \eta_k^\dagger \eta_k \rangle$ for forward and reverse bias is shown in Fig. S2(b)-(c). This reveals that in reverse bias most of the occupied eigenstates are the higher energy localized ones, while in forward bias there is significant occupation of lower energy

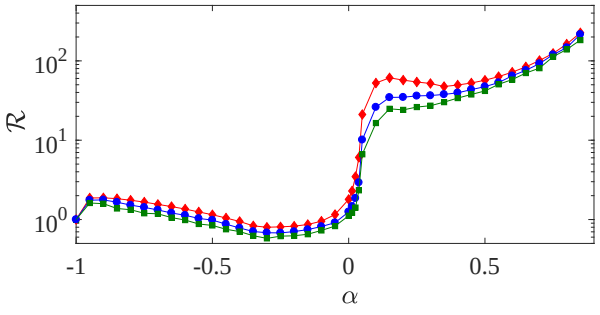

FIG. S1: (a) Rectification $\mathcal{R}$ as a function of α for $\phi = \pi$ (red $\diamond$), and average rectification sample over 100 samples of the phase picked from $\phi \in \pi + \pi/20[-1, 1]$ (blue $\circ$) and $\phi \in \pi + \pi/10[-1, 1]$ (green $\square$). Other parameters are $L = 1000$, $\lambda = 0.9$, $T_h = T_c + 1000$ and $T_c = 0.1$.

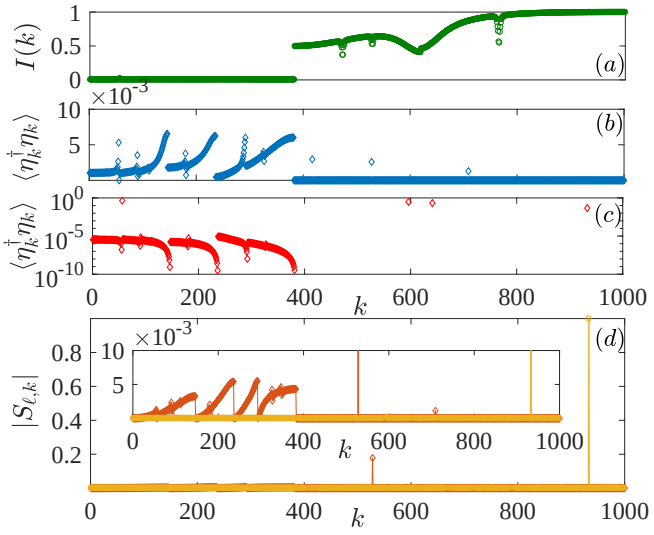

FIG. S2: (a) Inverse participation ratio $I(k)$ of the kth eigenmode of the Hamiltonian of Eq. (1) of the main paper. (b)-(c) Occupation probability of the eigenmodes k, $\langle \eta_k^\dagger \eta_k \rangle$, versus the mode number k ordered for increasing energy and for the (b) forward (in a lin-lin plot) and (c) reverse bias (in a log-lin plot). (d) Strength of the couplings $|S_{\ell,k}|$ of eigenmodes k to the left bath, i.e $\ell = 1$ (red $\diamond$), and right bath, $\ell = L$ (yellow $\circ$). The inset magnifies a portion of the y-axis to better show the coupling to delocalized modes. Common parameters are $\phi = \pi$, $T_h = 1000.1$, $T_c = 0.1$, $L = 1000$, $\lambda = 0.9$ and $\alpha = 0.9$.

delocalized eigenstates.

A deeper insight into the generation of such strong rectification via the mobility edge can be obtained by studying the strength of the coupling of each bath to the various k modes, i.e. $S_{\ell,k}$. In Fig. S2(d) we show $|S_{L,k}|$ versus k (yellow $\circ$) and $|S_{1,k}|$ (red $\diamond$). The inset is used to zoom in on the vertical axis so as to show the magnitude of $|S_{1,k}|$ for the delocalized modes. In Fig. S2(d) we observe that for $\phi = \pi$ the bath at site L is almost completely coupled only to one mode, which is localized at that edge. In fact there is a sharp peak for a high$-k$ mode which almost reaches unity. This also implies that the delocalized modes are very weakly coupled to this bath. For the bath at the first site, instead, $|S_{1,k}|$ is much more strongly coupled to delocalized modes. So the spatial position of the localized modes affects the strength of the coupling between a bath and the delocalized current-carrying modes. When connecting this with Eq. (4) of

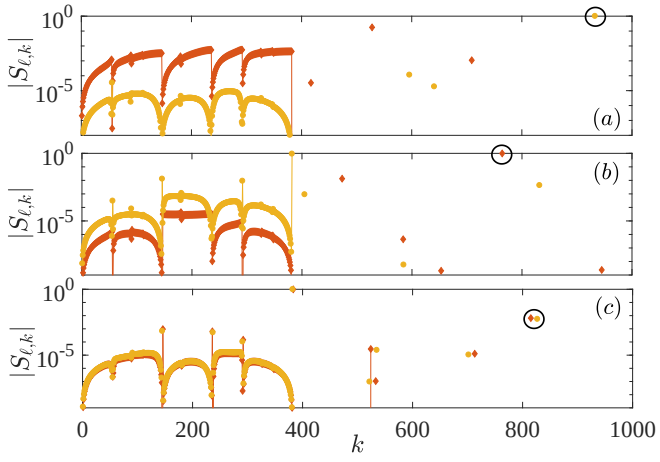

FIG. S3: (a-c) Strength of the couplings $|S_{\ell,k}|$ of eigenmodes k to the left bath, i.e $\ell = 1$ (red $\diamond$), and right bath, $\ell = L$ (yellow $\circ$), for (a) $\phi = \pi$, (b) 0 and (c) 1.07. The forward current, when compared to the reverse current, is larger in (a), lower in (b) and comparable in (c). Common parameters are $\lambda = 0.9$ and $\alpha = 0.9$. The black circles highlight the more strongly coupled localized modes.

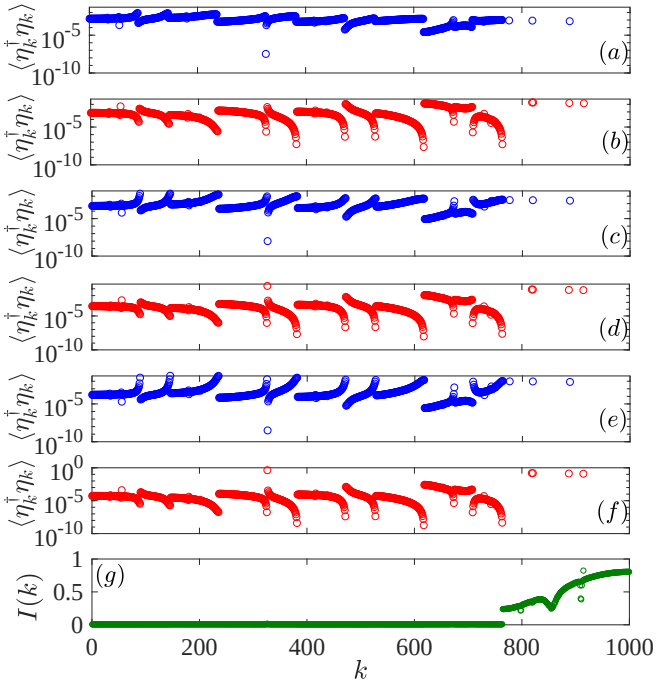

FIG. S4: (a)-(f) Occupation probability of the eigenmodes k, $\langle \eta_k^\dagger \eta_k \rangle$, versus the mode number k ordered for increasing energy. We consider $T_h = 10.1$ for the (a) forward and (b) reverse bias. We consider $T_h = 100.1$ for the (c) forward and (d) reverse bias. We consider $T_h = 1000.1$ for the (e) forward and (f) reverse bias. (g) Inverse participation ratio $I(k)$ of the kth eigenmode of the Hamiltonian. Common parameters are $L = 1000$, $\phi = \pi$, $T_c = 0.1$, $\lambda = 0.1$ and $\alpha = 0.9$.

the main paper, we observe that the interplay between the bosonic system and spin bath statistics, and the disparity in coupling strengths to the delocalized modes of the baths which together result in a significantly different current in the two biases.

By tuning the phase ϕ it is possible to move the localized modes and hence modify which bath is coupled to a localized mode. In Fig. S3 we show the coupling of the modes to the two baths $|S_{\ell,k}|$ for (a) $\phi = \pi$, (b) $\phi = 0$ and (c) $\phi = 1.07$. The three panels show the couplings to the bath at site $\ell = 1$ (red $\diamond$) and to the bath at site $\ell = L$ (yellow $\circ$). For Fig. S3(a) the current is stronger in forward bias, and in fact the coupling to the delocalized modes is stronger for the bath at site $\ell = 1$, while the bath at site $\ell = L$ there is a strong coupling to a single localized mode (highlighted by the black $\circ$) giving $\mathcal{R} \gg 1$. In Fig. S3(b) the situation for the couplings is inverted, so now there is a strong coupling to a single localized mode for the bath at site $\ell = 1$ (see within black $\circ$) and the bath at site $\ell = L$ is more strongly coupled to delocalized modes giving $\mathcal{R} \ll 1$. In Fig. S3(c) the coupling of localized and delocalized modes is similar for both baths, and it results that rectification is $\mathcal{R} \approx 1$.

III. ROLE OF TEMPERATURE IN MODES OCCUPATION

In Fig. S2 we have studied the occupation of the different k eigenmodes of the Hamiltonian in the steady state for a temperature difference $\Delta T = 1000$. Here we show how the occupation of the different modes is affected by the temperature difference. To show the generality of the effect we also consider different Hamiltonian parameters, namely $\alpha = 0.9$ and $\lambda = 0.1$. We study the occupation of all the modes $\langle \eta_k^\dagger \eta_k \rangle$ in Fig. S4 in forward (a),(c),(e) and reverse (b),(d),(f) bias. The localization of the modes is signalled by the modes' inverse participation ratio $I(k)$. For the parameters considered there is a clear transition between delocalized and localized modes around the mode $k = 765$. An increase in the hot temperature T_h is reflected in a larger occupation of the localized modes (which are at higher energy) and a lower occupation of the delocalized ones. This is particularly evident in reverse bias.

IV. MASTER EQUATION AND ROLE OF STATISTICS OF BATH IN RECTIFICATION

We consider the total Hamiltonian of system plus bath at sites $\ell = \{1, L\}$ as

$$H_T = H + \sum_{\ell=1,L} (H_{sS,\ell} + H_{S,\ell}) \,, \tag{S1}$$

where H is defined in the main paper, while the two spin baths are identical, except for the temperature T_ℓ, and have Hamiltonian $H_{S,\ell} = \sum_\nu \varepsilon_\nu \sigma^z_{\nu,\ell}/2$, where $\sigma^z_{\nu,\ell}$ is the

Pauli-z operator for the νth spin in the bath at site ℓ and ε_ν is its associated energy gap. The Hamiltonian that couples the system to a spin bath is taken as $H_{sS,\ell} = \sum_{\nu,\ell} g_\nu (a_\ell + a_\ell^\dagger)(\sigma_{\nu,\ell}^+ + \sigma_{\nu,\ell}^-)$, where g_ν is the coupling strength of νth spin in the bath to its respective boundary site ℓ, assumed to be identical for both, and $\sigma_{\nu,\ell}^\pm$ are its corresponding raising and lowering operators.

In terms of the eigenoperators of the system Hamiltonian, we can write $H_{sS,\ell} = \sum_{\alpha\omega} A_{\ell,\alpha}(\omega) \otimes B_{\ell,\alpha}$, where $A_{\ell,\alpha}(\omega)$ and $B_{\ell,\alpha}$ respectively act on the system and on the bath. The operator $A_{\ell,\alpha}(\omega)$ is chosen to satisfy

$$[H, A_{\ell,\alpha}(\omega)] \;=\; -\omega A_{\ell,\alpha}(\omega) \tag{S2}$$

Note that, after rotating wave approximation, α takes two values with $A_{\ell,1}(\omega) = \sum_k S_{\ell,k}\eta_k \delta_{\omega,+\epsilon_k}$, $A_{\ell,2}(\omega) = \sum_k S_{\ell,k}^* \eta_k^\dagger \delta_{\omega,-\epsilon_k}$, while $B_{\ell,1} = \sum_\omega g_{\ell,\omega}\sigma_{\omega,\ell}^+$ and $B_{\ell,2} = \sum_\omega g_{\ell,\omega}\sigma_{\omega,\ell}^-$. For the above thermal bath coupling, the steady state can be obtained from the Lindblad dissipator [1]

$$\begin{aligned} D_\ell(\rho(t)) \;=\; & \sum_{\omega,\alpha} \Gamma_{\ell,\alpha}(\omega)[A_{\ell,\alpha}(\omega)\rho(t)A_{\ell,\alpha}^\dagger(\omega) \\ & -\frac{1}{2}\{A_{\ell,\alpha}^\dagger(\omega)A_{\ell,\alpha}(\omega), \rho(t)\}], \end{aligned} \tag{S3}$$

with

$$\Gamma_{\ell,\alpha}(\omega) = \int_0^\infty dt\; e^{i\omega t}\mathrm{Tr}_B[B_{\ell,\alpha}^\dagger(\tau)B_{\ell,\alpha}(0)\rho_{S,\ell}]. \tag{S4}$$

Here $\rho_{S,\ell} = \exp(-\beta_\ell H_{S,\ell})/Z$ is the thermal state of the bath coupled to site ℓ at inverse temperature $\beta_\ell = 1/T_\ell$ and $Z = \mathrm{tr}\left[\exp(-\beta_\ell H_{S,\ell})\right]$. Thus,

$$\Gamma_{\ell,1}(\omega) \;=\; J_\ell(\omega)(1 - n_S(\beta_\ell\omega)). \tag{S5}$$

where $n_S(\beta_\ell\omega) = \left(e^{\beta_\ell\omega}+1\right)^{-1}$ is the spin occupation factor for the bath coupled to site ℓ, and $J(\omega) = \sum_\nu |g_\nu|^2\pi\delta(\omega-\varepsilon_\nu)$ is the spectral density identical for both baths. Similarly

$$\Gamma_{\ell,2}(\omega) \;=\; J(-\omega)n_S(-\beta_\ell\omega). \tag{S6}$$

For any operator O the dissipator evolution is

$$\begin{aligned} D_\ell(O) \;=\; & \sum_{\epsilon_k} |S_{\ell,k}|^2 J(\epsilon_k)\Big[n_S(\beta_\ell\epsilon_k)\big[\eta_k O\eta_k^\dagger - \frac{1}{2}\{\eta_k\eta_k^\dagger, O\}\big] \\ & +(1-n_S(\beta_\ell\epsilon_k))\big[\eta_k^\dagger O\eta_k - \frac{1}{2}\{\eta_k^\dagger\eta_k, O\}\big]\Big]. \end{aligned} \tag{S7}$$

In the steady state limit, $\sum_\ell D_\ell(O) = 0$, as expected. Thus, the steady state single-particle density matrix $\langle\eta_k^\dagger\eta_q\rangle$ is

$$\langle\eta_k^\dagger\eta_q\rangle = \delta_{k,q}\frac{\sum_\ell |S_{\ell,k}|^2 n_S(\beta_\ell\epsilon_k)}{\sum_\ell |S_{\ell,k}|^2\left[1-2n_S(\beta_\ell\epsilon_k)\right]}. \tag{S8}$$

The thermal current is given by the energy exchange with each bath which in steady state needs to be opposite. Hence we get

$$\begin{aligned} \mathcal{J} \;&=\; \mathrm{Tr}\{HD_1(\rho)\} = -\mathrm{Tr}\{HD_L(\rho)\}, \\ &=\; \sum_{\epsilon_k>0} \epsilon_k |S_{1,k}|^2 |S_{L,k}|^2 J(\epsilon_k) \\ &\qquad \times \frac{n_S(\beta_1\epsilon_k) - n_S(\beta_L\epsilon_k)}{\sum_\ell |S_{\ell,k}|^2(1-2n_S(\beta_\ell\epsilon_k))}. \end{aligned} \tag{S9}$$

Suppose we use bosonic bath instead of spins with a different system-bath coupling term $H_{sB,\ell} = \sum_\nu g_\nu(a_\ell + a_\ell^\dagger)(b_{\nu,\ell} + b_{\nu,\ell}^\dagger)$, in terms of bath bosonic creation $b_{\nu,\ell}^\dagger$ and annihilation $b_{\nu,\ell}$ operators for the νth mode of the bath at site ℓ. In this case the bath Hamiltonian is given by $H_{B,\ell} = \sum_\nu \varepsilon_\nu\; b_{\nu,\ell}^\dagger b_{\nu,\ell}$. Following the above steps, we get $\Gamma_{\ell,1}(\omega) = J(\omega)[1+n_B(\beta_\ell\omega)]$ and $\Gamma_{\ell,2}(\omega) = J(-\omega)n_B(-\beta_\ell\omega)$, where $n_B(\beta_\ell\omega) = \left(e^{\beta_\ell\omega}-1\right)^{-1}$ is the Bose-Einstein distribution. Hence, the occupation of each k eigenmode when the system is coupled to the two bosonic baths is

$$\langle\eta_k^\dagger\eta_k\rangle = \frac{\sum_\ell |S_{\ell,k}|^2 n_B(\beta_\ell\epsilon_k)}{\sum_\ell |S_{\ell,k}|^2}, \tag{S10}$$

and the steady state thermal current is

$$\begin{aligned} \mathcal{J} \;&=\; \mathrm{Tr}\{HD_1(\rho)\} = -\mathrm{Tr}\{HD_L(\rho)\}, \\ &=\; \sum_k \frac{\epsilon_k |S_{1,k}|^2 |S_{L,k}|^2 J(\epsilon_k)}{\sum_\ell |S_{\ell,k}|^2} \\ &\qquad \times[n_B(\beta_1\epsilon_k) - n_B(\beta_L\epsilon_k)]. \end{aligned} \tag{S11}$$

Thus, it follows that a bosonic system connected to bosonic baths gives no rectification, whereas a rectifying effect can be obtained using spin baths.

[1] H.-P. Breuer, and F. Petruccione, *The Theory of Open Quantum Systems* (Oxford University Press, Oxford, 2007).